



**HAL**  
open science

# In-Depth Study of Cyclodextrin Complexation with Carotenoids toward the Formation of Enhanced Delivery Systems

Sébastien Clercq, Feral Temelli, Elisabeth Badens

► **To cite this version:**

Sébastien Clercq, Feral Temelli, Elisabeth Badens. In-Depth Study of Cyclodextrin Complexation with Carotenoids toward the Formation of Enhanced Delivery Systems. *Molecular Pharmaceutics*, 2021, 18 (4), pp.1720-1729. 10.1021/acs.molpharmaceut.0c01227 . hal-03600451

**HAL Id: hal-03600451**

**<https://hal.science/hal-03600451v1>**

Submitted on 7 Mar 2022

**HAL** is a multi-disciplinary open access archive for the deposit and dissemination of scientific research documents, whether they are published or not. The documents may come from teaching and research institutions in France or abroad, or from public or private research centers.

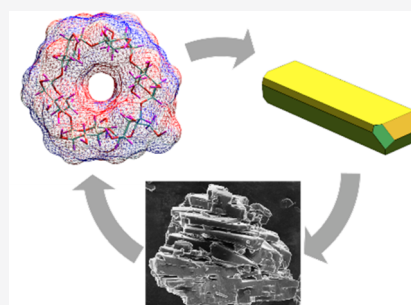
L'archive ouverte pluridisciplinaire **HAL**, est destinée au dépôt et à la diffusion de documents scientifiques de niveau recherche, publiés ou non, émanant des établissements d'enseignement et de recherche français ou étrangers, des laboratoires publics ou privés.

# In-Depth Study of Cyclodextrin Complexation with Carotenoids toward the Formation of Enhanced Delivery Systems

Sébastien Clercq, Feral Temelli, and Elisabeth Badens

**ABSTRACT:** The goal of this study was molecular modeling of cyclodextrin (CD) and carotenoid complex formation. Distinction was made between complexes resulting from interactions between carotenoids and either molecularly dispersed CDs or solid crystalline CDs, considering that both cases can occur depending on the complex formation process pathways. First, the formation of complexes from dispersed CD molecules was investigated considering five different CDs ( $\alpha$ CD,  $\beta$ CD, methyl- $\beta$ CD, hydroxypropyl- $\beta$ CD, and  $\gamma$ CD) and lutein, as a model carotenoid molecule. The interactions involved and the stability of the different complexes formed were evaluated according to the CD size and steric hindrance. Second, the formation of complexes between four different crystalline CDs ( $\beta$ CD with three different water contents and methyl- $\beta$ CD) and three carotenoid molecules (lutein, lycopene, and  $\beta$ -carotene) was studied. The docking/adsorption of the carotenoid molecules was modeled on the different faces of the CD crystals. The findings highlight that all the CD faces, and thus their growth rates, were equally impacted by the adsorption of the carotenoids. This is due to the fact that all the CD faces are exhibiting similar chemical compositions, the three studied carotenoid molecules are rather chemically similar, and last, the water-carotenoid interactions appear to be weak compared to the CD-carotenoid interactions.

**KEYWORDS:** cyclodextrin, complexation, delivery systems, molecular modeling, adsorption



## 1. INTRODUCTION

Cyclodextrins (CDs) are used extensively in the food, pharmaceutical, and cosmetic industries as delivery vehicles for aromas, flavors, bioactives, and drugs. These cyclic oligosaccharides are obtained from starch by enzymatic treatment and contain six, seven, or eight ( $\alpha$ ,  $\beta$ , or  $\gamma$ CD, respectively) D-glucopyranose units linked by  $\alpha(1-4)$  glycosidic bonds, which leads to the hollow, truncated-cone shape of the cyclodextrin molecule. The primary and secondary hydroxyl groups are located on the narrow and wide edges, respectively, of the truncated cone.<sup>1</sup> Even though these “natural” cyclodextrins are hydrophilic molecules, their solubility in water is somewhat limited, especially for  $\beta$ CD,<sup>2</sup> which is considered mainly to be due to the relatively strong binding between cyclodextrin molecules in the crystal state.<sup>1</sup> Their relatively high crystal lattice energy also leads to their high melting points (240 to 265 °C).<sup>1</sup> In addition, the presence of intramolecular hydrogen bonding within the cyclodextrin molecule, especially between the hydroxyl groups in the C-2 and C-3 positions of adjacent glucopyranose units and the oxygen of the glycosidic bond, helps stabilize the overall structure, while preventing hydrogen bond formation with surrounding water molecules.<sup>1</sup> Thus, the central cavity is considered to be hydrophobic, with a polarity similar to that of aqueous ethanolic solution.<sup>1</sup> Sabadini et al.<sup>2</sup> reported that 6.4, 9.6, and 14.2 water molecules are present in the stable hydrates

of  $\alpha$ CD,  $\beta$ CD, and  $\gamma$ CD lattices, respectively, of which 2, 6, and 8.8 water molecules are inside the cavity. More recently, a thermodynamic approach<sup>3</sup> highlighted a higher theoretical stability of  $\beta$ CD hydrates when the crystal is fully loaded with water molecules, which corresponds to 12 water molecules and above. Crini et al.<sup>4</sup> specified the number of water molecules within the cavity as 6–8, 11–12, or 13–17 for  $\alpha$ ,  $\beta$ , or  $\gamma$ CD, respectively.

Crystalline forms of native cyclodextrins have been classified as cage- or channel-type, with the cage-type structures having herringbone- or brick-type categories.<sup>5</sup> Herringbone-type crystals typically form when hydrates of  $\alpha$ ,  $\beta$ , or  $\gamma$ CD are crystallized.<sup>6</sup> Crystalline solids can be converted to an amorphous mixture after random substitution of hydroxyl groups, enhancing their solubility in water (for example, methyl (M)- or hydroxypropyl(HP)-CD). Random substitution results in a mixture of isomers with different levels of substitution and different molecular weights, which decreases their ability to form crystalline aggregates.<sup>7</sup>

The use of cyclodextrins as a carrier for a wide range of hydrophobic bioactives/drugs depends on the formation of inclusion complexes between the cyclodextrin and the bioactive, based on an association/dissociation equilibrium between the free components and the complex. If the size of the bioactive molecule is compatible with that of the cyclodextrin cavity, the complex formed is strong. Noncovalent interactions are important to form such complexes, including van der Waals forces, electronic effects, and hydrophobic interactions.<sup>6</sup> Examples of such inclusion complexes include black pepper oleoresin,<sup>8</sup> essential oils of clove<sup>9</sup> and sweet orange,<sup>10</sup> saffron anthocyanins,<sup>11</sup> and different types of antioxidants (stilbenes, fat-soluble vitamins, carotenoids, and coenzyme Q10) as reviewed by López-Nicolás et al.<sup>12</sup> Carotenoids such as  $\beta$ -carotene, lycopene, and lutein have received growing attention because of their antioxidant activity and demonstrated health benefits, especially in relation to protection against cardiovascular diseases and different types of cancer or other disorders, including lycopene against prostate cancer<sup>13</sup> and lutein against age-related macular degeneration.<sup>14</sup> As hydrophobic molecules, the incorporation of carotenoids into aqueous-based formulations is very challenging, and they are sensitive to heat, light, and oxygen; therefore, the use of cyclodextrins as delivery vehicles has been attempted.<sup>12</sup> The conventional methods employed for the preparation of such complexes include spray drying, freeze-drying, coevaporation, sealed-heating, and kneading.<sup>15–17</sup> With the latest developments in supercritical carbon dioxide (SC-CO<sub>2</sub>) technology for the different approaches to particle formation,<sup>18</sup> various techniques have been applied for the encapsulation of carotenoids; however, their complexation with cyclodextrin under a SC-CO<sub>2</sub> environment has not been reported. Developing such novel approaches requires a better understanding of the interactions between cyclodextrins and carotenoids.

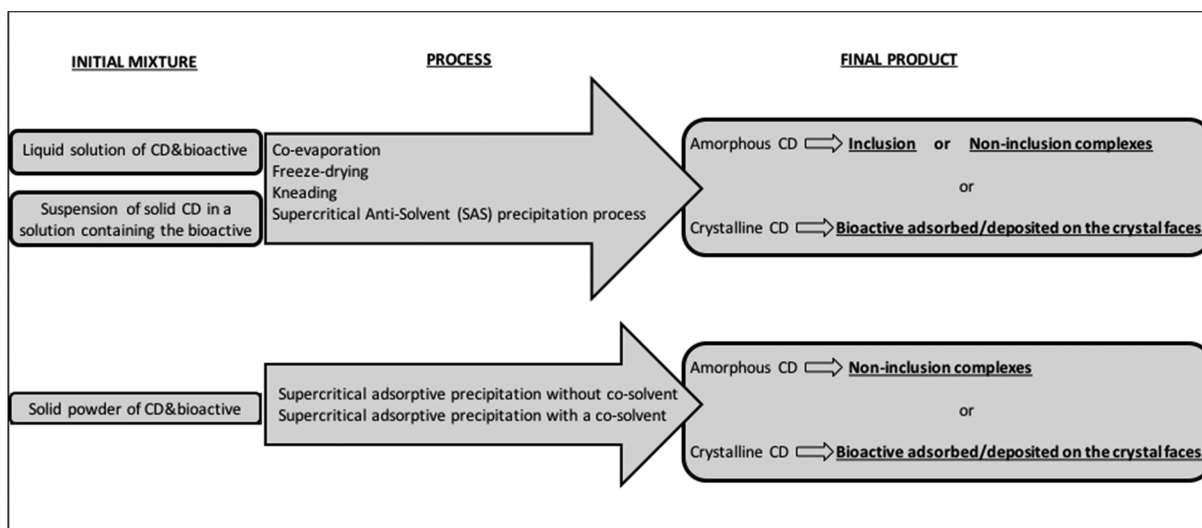
In addition to the inclusion complexes mentioned above, the fact that cyclodextrins can form noninclusion complexes as well as self-assemble into aggregates and nano-/microparticles in aqueous solutions has been reported.<sup>7,19,20</sup> Self-association of cyclodextrin complexes was observed by many authors and verified by different analytical and microscopy techniques as reviewed by Loftsson et al.<sup>20</sup> and He et al.,<sup>6</sup> respectively. In addition to hydrophobic interactions, the hydroxyl groups (especially the secondary hydroxyl groups) of cyclodextrins play an important role in the formation of such aggregates and complexes via hydrogen bond formation with other molecules of cyclodextrin or bioactive. The formation of such aggregates, leading to increased opalescence with time followed by precipitation presents a major challenge for some applications, especially in eye drops or other ophthalmic formulations.<sup>21</sup> Different types of natural cyclodextrins displayed different aggregation kinetics, while the use of modified cyclodextrins (*M*- $\beta$ CD and *HP*- $\beta$ CD) led to minimal aggregation.<sup>19</sup>

Over roughly the past 25 years, different researchers have investigated cyclodextrin/drug complexes using molecular modeling approaches. Loftsson et al.<sup>21,22</sup> have indicated that computer modeling of cyclodextrin complexes ignores the presence of noninclusion complexes and that the models employed tend to oversimplify the behavior especially in concentrated, nonideal solutions. They also highlighted the discrepancies in the literature for the stability constants of some cyclodextrin/drug complexes in dilute solutions, even though the results are expected to be similar under such an

ideal scenario. The products are referred to as an “inclusion complex” even though the form of cyclodextrin is not well characterized in many studies. As well, the actual size of the cyclodextrin cavity should be considered, which is only 5.3/4.7, 6.5/6.0, and 8.3/7.5 Å in external/internal diameter for  $\alpha$ ,  $\beta$ , and  $\gamma$ CD, respectively.<sup>4</sup> Some modeling approaches depict cyclic rings of some drugs to be inserted into the cavity,<sup>1</sup> which is physically not possible considering the drug steric hindrance. For such a case, molecular modeling showed the lowest energy to be associated with 2:1 *M*- $\beta$ CD/lutein ratio with the two hexatomic ring ends of lutein inserted into the cavities of two *M*- $\beta$ CD molecules.<sup>23</sup> As well, using both experimental and molecular dynamic simulation approaches, Zhao et al.<sup>24</sup> showed that among  $\alpha$ CD,  $\beta$ CD,  $\gamma$ CD, and *HP*- $\beta$ CD, lutein solubility in distilled water was the highest with *HP*- $\beta$ CD, which was in good agreement with their simulations, showing that lutein interacts more strongly with the latter.

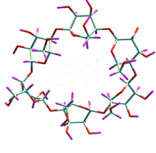
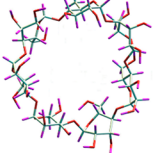
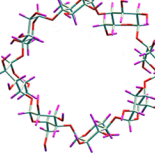
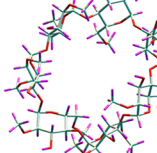
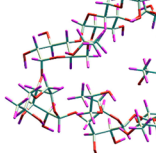
The study of noninclusion complexes aims for a better understanding of host–guest interactions with cyclodextrins through molecular modeling calculations at thermodynamic equilibrium. A computational study allows one to decipher atom-scale physics, such as steric hindrances or favored intermolecular interactions, that drive macroscopic phenomenon. Faucci et al.<sup>25</sup> used predictive molecular modeling, based on the AMBER force field, to investigate a drug (econazole) and  $\alpha$ CD interactions in the presence of malic acid. Based on systematic research of minimal energy conformations of the molecular system, they proposed a mechanism that rationalizes the formation of the multicomponent complexes: a repeated concatenation of the three-component assembly, nested in a specific conformation of the three elements. Such computational tools are therefore a great asset to accelerate the development of new systems with targeted properties, such as enhanced bioavailability of the drug. Zhao et al.<sup>24</sup> addressed the issue of the low-bioavailability of lutein as well as its insufficient loading with the different types of cyclodextrins by using a molecular modeling approach also with the force field package AMBER. The authors showed that the presence of given polymers enabled bridged interactions between lutein and  $\gamma$ CD, so much so that the quality of the multicomponent formulation allowed for an increased bioavailability of the lutein. The molecular mechanics approach is therefore a powerful asset to perform a rapid screening of intermolecular interactions and directs the experimental investigation to those conditions that have the best theoretical potential. For instance, a host–guest screening performed by Nalawade and Gajjar<sup>23</sup> highlighted the disparity of the interaction strength depending on the considered cyclodextrin, with *M*- $\beta$ CD and *HP*- $\beta$ CD seemingly providing higher interactions with lutein than  $\beta$ CD.

In summary, a detailed review of all the literature references related to CD/bioactive complexes demonstrated that their characteristics depend on the preparation method as well as on the bioactive and CD molecule dimensions and their chemical affinities. Concerning the influence of the preparation method, the pathway followed during the process is critical. If the cyclodextrin remains in a solid crystalline form during all the different processing steps, the bioactive/drug will have interactions only with the cyclodextrin molecules or their constitutive atoms that are on the different crystal faces. By contrast, if the cyclodextrin is dispersed in a fluid phase at any step of the process, the crystal may have dissolved, and it is possible for the bioactive to form an inclusion complex or a



**Figure 1.** Overview of the different characteristics of CD/bioactive complexes depending on the initial mixture state and on the process employed.

**Table 1. Properties of the Various Types of Cyclodextrins Considered**

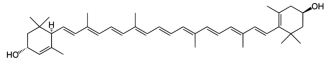
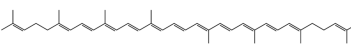
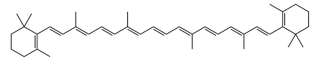
Type of cyclodextrin	$\alpha$ CD	$\beta$ CD	$\gamma$ CD	M- $\beta$ CD	2-HP- $\beta$ CD
Chemical formula	$C_{36}H_{60}O_{30}$	$C_{42}H_{70}O_{35}$	$C_{48}H_{80}O_{40}$	$C_{54}H_{94}O_{35}$	$C_{63}H_{112}O_{42}$
Molecular model					
Number of glucopyranose units	6	7	8	7	7
Molar mass (g/mol)	972.9	1135.0	1297.1	1303.3	1541.5
Central cavity diameter (Å)	4.7 – 5.3 [4]	6.0 – 6.5 [4]	7.5 – 8.3 [4]	5.8–6.5 [34]	6.0 [34]
Water solubility at 25°C (g/L)	145 [4]	18.5 [4]	232 [4]	>500 [34]	>1200 [34]
Melting temperature (°C)	277.8 (decompose) [30]	267.5 – 269.3 [31]	287 [32]	296.8 [33]	278 [35]

noninclusion complex with individual cyclodextrin molecules or their aggregates. Therefore, it is critical to have a good understanding of the behavior of CD throughout the process to achieve the targeted functionality.

Figure 1 summarizes the different characteristics of CD/bioactive complexes that can be formed depending on the process used and on the initial state of the CD+bioactive mixture. When coevaporation is used, both CD and bioactive/drug are dissolved in water or organic solvent. In that case, it is possible to form either inclusion or noninclusion complexes or CD crystals with the drug being deposited on the crystalline faces. For the kneading process, a partial amorphization can be observed when a mixture of water and ethanol is used.<sup>15–17</sup> The formation of inclusion or noninclusion complexes is then possible. During the sealed-heating process, employing a static step in the presence of water at a given temperature, for example 75 °C,<sup>15–17</sup> the final product may remain crystalline.

Regarding the different processes using supercritical fluids, and particularly SC-CO<sub>2</sub>, two main types of processes can be used for loading cyclodextrins with a bioactive: supercritical anti-solvent (SAS) precipitation or adsorptive precipitation.<sup>26</sup> The SAS precipitation can be carried out starting from either a liquid solution of CD and bioactive/drug or a suspension of CD crystals in a liquid solution containing the bioactive/drug. In the former case, it is possible to form all the different types of complexes. In the latter case, only CD crystalline powder with a bioactive/drug deposit can be obtained. Lastly, when adsorptive precipitation is performed, only the bioactive is solubilized in the SC-CO<sub>2</sub>. During this process, first there is adsorption of the bioactive onto the CD crystal faces. Then, during the depressurization step, upon release of CO<sub>2</sub>, there is supersaturation of the bioactive/drug, which precipitates on the CD particles.<sup>15–18,27–29</sup> In addition, solid phase transformation may also possibly happen under

**Table 2. Properties of Lutein, Lycopene, and  $\beta$ -Carotene**

	Lutein	Lycopene	$\beta$ -Carotene
Chemical formula	$C_{40}H_{56}O_2$	$C_{40}H_{56}$	$C_{40}H_{56}$
Molecule			
Molar mass (g/mol)	568.9	536.9	536.9
Melting temperature ( $^{\circ}C$ ) [36]	196	175	183
Water solubility	Insoluble	Insoluble	Insoluble
BCS* Class	Class II	Class II	Class II

\*Biopharmaceutics classification system; class II = high permeability and low solubility.

pressure, and in that case, amorphization of the CD can be observed.<sup>17</sup>

In the main context of cyclodextrin and carotenoid complex formation, the overall objective of this study was to use molecular modeling as a tool for the screening of different types of cyclodextrins ( $\alpha$ ,  $\beta$ , or  $\gamma$ CD) and their methyl- and hydroxypropyl derivatives, described in Table 1) and bioactives (the carotenoids  $\beta$ -carotene, lycopene, and lutein selected as a model class of bioactives, described in Table 2) in an effort to select the best CD/carotenoid combination for further development.

Based on the previous reports discussed above, the modeling work has two distinct parts. The first part deals with the modeling of the interactions between dispersed cyclodextrin and lutein so as to identify the structure of the most stable CD/lutein complex. This would be useful in the case of the formation of complexes using a preparation method, involving the dispersion at the molecular state of excipient and bioactive. In the second part of this study, the modeling of the crystal lattice structure has been performed where the CD crystal has been further built *in vacuo* (without considering any environment). Lastly, the docking of the three selected carotenoids onto the different excipient crystal faces has been investigated. This last part allows prediction of the characteristics of the complexes that are formed when the crystalline CD remains solid throughout the preparation method, leading then to the deposition of bioactive onto CD particle surfaces and their pores if there are any.

## 2. MOLECULAR MODELING METHODOLOGY

The following molecular modeling work has been conducted with the molecular modeling—quantum modeling software GenMol. The GenMol package has its own custom force field derived from MM2 and defines the atomic charges using the Del Re method.<sup>37–39</sup>

A molecule or a group of molecules—a system—can be modeled using solely the structural formulas of molecules. The addition of each atom, or group of atoms, is followed by a global refinement in an effort to obtain an optimized system *in vacuo*, i.e. a system with the lowest energy, and by considering steric hindrances. This method leads to an *in-vacuo* optimized system, which can be used for docking or calculation of intermolecular interactions. The molecular conformation is optimized in several steps of reducing its energy ( $E_{mol}$ ) by lowering the bonding strains as well as the nonbonding interactions:

$$E_{mol} = \sum E_S + \sum E_B + \sum E_T + \sum E_{vdW} + \sum E_C + \sum E_H \quad (1)$$

where  $E_S$  is the stretching energy,  $E_B$  is the bending energy,  $E_T$  is the torsion energy,  $E_{vdW}$  is the van der Waals energy,  $E_C$  is the Coulombic (or electrostatic) energy, and  $E_H$  is the hydrogen energy.  $E_S$ ,  $E_B$ , and  $E_T$  are bonding, intramolecular energies, calculated for each pair of bonded atoms using MM2 potentials, whereas  $E_{vdW}$ ,  $E_C$ , and  $E_H$  are nonbonding interaction energies, calculated for each nonbonded pair of atoms separated by at least two atoms in between (1–4 relationship and more). Lennard-Jones potentials are used for  $E_{vdW}$  and  $E_C$ . This refinement of the molecular conformation is performed *in vacuo* by only considering intramolecular interactions and without considering any neighboring molecules.

The second way of building a system is by using online databanks such as the Cambridge Structural Databank (CSD). The CSD compiles structures retrieved from crystal or powder diffraction analysis into CIF files, hence providing the position of atoms in the crystal cell as well as the crystal lattice parameters and space group, among others. This method is used for building molecules into crystals and has been applied in the second part of this work for the study of the docking of carotenoids onto cyclodextrin crystals.

The crystal is built according to the attachment energy formalism,<sup>40</sup> which allows retrieval of the crystal habit by calculating the so-called Attachment Energy ( $E_{att-hkl}$ ) for every one of the ( $hkl$ ) faces. This energy is proportional to the energy released through the deposition of a whole slice of molecules in the [ $hkl$ ] direction. The attachment energy is therefore calculated individually for each ( $hkl$ ) face. To do so, the software computes the intermolecular interaction energy between a deposited slice and the rest of the crystal.

Once every one of the  $E_{att-hkl}$  has been calculated, the crystal habit can be drawn thanks to a simple proportional correlation:

$$V_{hkl} \propto |E_{att-hkl}| \quad (2)$$

where  $V_{hkl}$  is the linear growth rate of the ( $hkl$ ) face. Logically, the slow growing faces, namely the ones most likely to have a high surface area, are the ones with the highest  $E_{att-hkl}$ ; in other words, the ones that release the highest amount of energy during the growth are therefore the most stable faces.

## 3. RESULTS

**3.1. Modeling of Noninclusion Complexes.** In the first part, lutein was considered as a model carotenoid molecule,

because it possesses all of the chemical groups of interest, namely a carbonated chain, methyl groups, a cyclohexyl head, and a hydroxyl group on both extremities. However, different cyclodextrins of different sizes and ramifications were evaluated. The five studied cyclodextrins were  $\alpha$ ,  $\beta$ , M- $\beta$ , 2-HP- $\beta$ , and  $\gamma$ CD. They have been built from their chemical formulas (Table 1) and optimized *in vacuo*.

As a fundamental investigation of carotenoid and cyclodextrin interactions, solvent molecules were not considered in this work. A screening of the interaction energy calculation was conducted with cyclodextrins interacting with four different areas of the lutein molecule, corresponding to different chemical groups. The cyclodextrin was manually placed close to the chosen area. Figure 2 presents the four chosen docking sites.

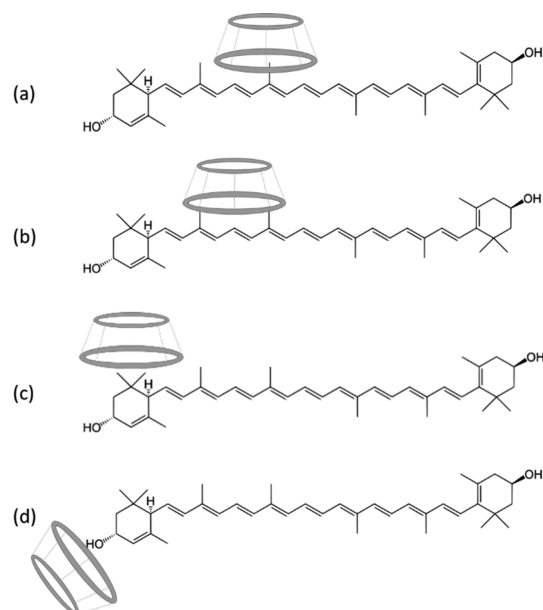


**Figure 2.** Scheme of the imposed docking positions of cyclodextrins on the lutein molecule, on (a) the central-most methyl group, (b) two successive methyl groups, (c) the dimethyl group on the cyclic head, and (d) the hydroxyl group.

All simulations were composed of 5000 cycles of optimization computed in order to reduce the energy of the systems. Each cycle of optimization consisted of a mild shaking, leading to a random displacement of atoms within a short-range, followed by an optimization around pivots, with all pivots being considered simultaneously and resolved through a genetic algorithm, followed by an optimization using conjugated gradients finalized by a conformational analysis. A new optimum was found when the overall energy was lower than the previous optimal system. By using this method, the optimizer is not parametrized so as to work on the whole molecular surface of lutein, whose size would make the calculation either very long or less likely to find the best docking spot. This approach allows the optimizer to dig further into finding the best docking site in its specific area compared with full-size docking and has concomitantly allowed a 15-fold acceleration compared with the classical docking algorithm. A 3D modeling of the simulation outcome is given in Figure 3.

Each final system resulted in a pair of molecules optimized with one another in order to maximize the interaction energy,  $E_i$ , expressed in kcal/mol.  $E_i$  is calculated as a sum of the three

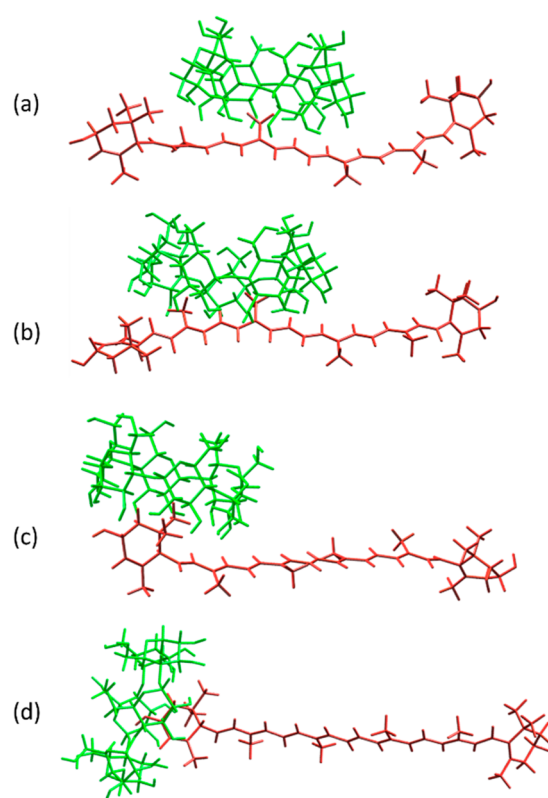


**Figure 3.** Outcome of the docking of  $\alpha$ CD on lutein with imposed areas: (a) one methyl group, (b) two successive methyl groups, (c) dimethyl group, and (d) hydroxyl group.

intermolecular interactions,  $E_{vdW}$ ,  $E_C$ , and  $E_H$ , with  $E_{vdW}$  being preponderant. Resulting  $E_i$  values are presented in Table 3.

**Table 3.** Interaction Energies ( $E_i$ , kcal/mol) of Cyclodextrins and Lutein in Different Areas

	(a) Methyl group	(b) Two successive methyl groups	(c) Dimethyl group	(d) Hydroxyl group
$\alpha$ CD	-19.65	-16.64	-14.96	-12.09
$\beta$ CD	-16.91	-21.24	-19.8	-20.34
2 $\times$ $\beta$ CD <sup>a</sup>	-19.3	-21.2	-20.0	-19.9
M- $\beta$ CD	-12.38	-20.22	-22.43	-23.2
HP- $\beta$ CD	-16.54	-19.79	-21.12	-23.48
$\gamma$ CD	-19.89 <sup>b</sup>	-15.69	-19.36	-14.56

<sup>a</sup>2 $\times$   $\beta$ CD refers to having two  $\beta$ CD molecules interacting with lutein.  
<sup>b</sup> $\gamma$ CD slid to a position similar to that of (c).

The calculated  $E_i$  values highlight an important disparity of behavior between different cyclodextrins, indicating that each cyclodextrin interacts differently with each docking site. As the smallest molecule in this list,  $\alpha$ CD has the strongest interactions with one methyl group of the polyene chain. Its small dimension prevents a good fit with two successive methyl groups or a dimethyl group, as well as properly circling the polar head. As a result, the steric hindrance creates a distance that significantly lowers  $E_{vdW}$ , which is the predominant interaction force, therefore lowering the global  $E_i$ . Figure 4 exhibits the low fitting of  $\alpha$ CD around the cyclic head of lutein,

while Figure 5 exhibits the best fit of  $\alpha$ CD with lutein, namely close to a methyl group.

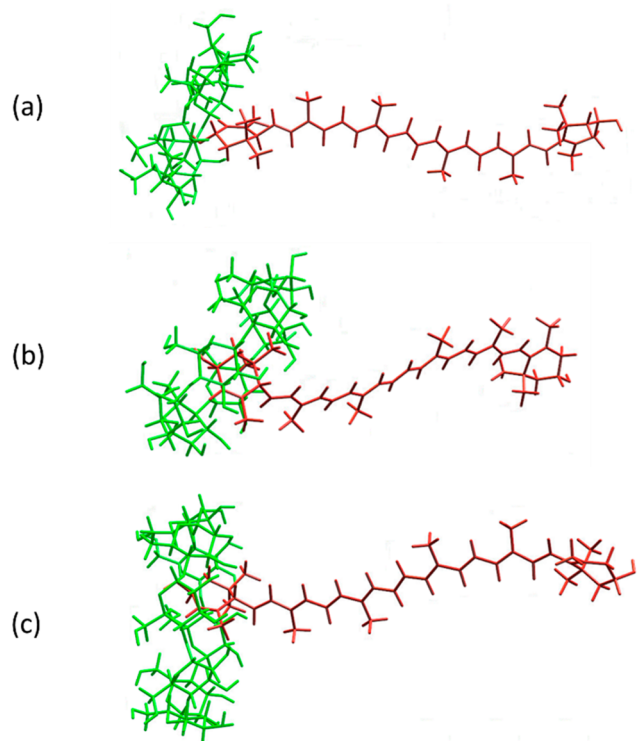


Figure 4. (a)  $\alpha$ CD, (b)  $\beta$ CD, and (c)  $\gamma$ CD interacting with the extremity of lutein.

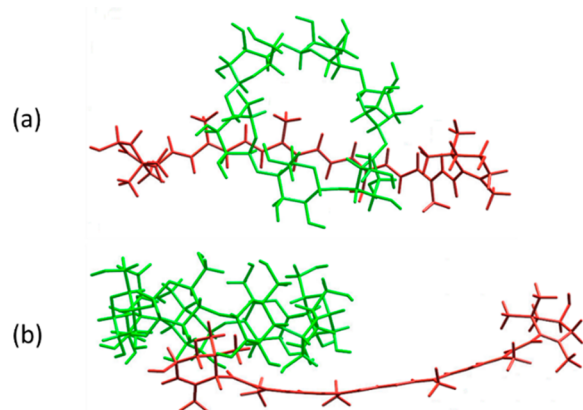


Figure 5. (a)  $\alpha$ CD vs methyl and (b)  $\gamma$ CD vs dimethyl groups, representing the respective best result.

With 7 glucopyranoside units,  $\beta$ CD, M- $\beta$ CD, and HP- $\beta$ CD are fitting well with two successive methyl groups and the dimethyl group as well as with the cyclic head. As shown in Figure 4b, the size of their inner core is matching the size of the cyclic head of lutein, which enhances van der Waals interactions. Consequently, in contrast to  $\alpha$ CD, lower intermolecular interactions were calculated with one methyl group of lutein. Those results are in agreement with the findings of Nalawade and Gajjar (2015). Both M- $\beta$ CD and HP- $\beta$ CD interact more strongly with lutein compared to  $\beta$ CD. The configuration is more energetically favored when  $\beta$ CD—or its ramified derivatives M- $\beta$ CD and HP- $\beta$ CD—is oriented

perpendicularly to the lutein molecule and is situated next to a cyclic head, which was also reported by Nalawade and Gajjar.<sup>23</sup>

Finally, with an extra glucopyranoside unit,  $\gamma$ CD is too large to closely fit around the extremity of lutein. As can be seen in Figure 4, empty space remains within the cyclodextrin cavity. Hence, a couple of glucopyranoside units are too distant from the atoms of the lutein extremity and only generate reduced  $E_{vdW}$ . The best fit for  $\gamma$ CD is, however, close to the cyclic head. Indeed,  $\gamma$ CD has the highest interaction along the dimethyl group, almost in parallel with the cyclic head, which is illustrated in Figure 5. Given its larger size,  $\gamma$ CD also interacts with the first methyl group. The absolute value of this interaction is still lower than those calculated for  $\beta$ CD, M- $\beta$ CD, and HP- $\beta$ CD and their respective best fit.

Furthermore, the cyclodextrin complex with lutein is inevitably a noninclusion complex, as one lutein molecule is many times larger than the largest studied cyclodextrin,  $\gamma$ CD. Size scales also allow for a 2:1 CD/lutein complex. According to the showcased modeling results, a  $\beta$ CD and lutein mixture could possibly result in a 2:1 noninclusion complex with the two cyclodextrins being located either at both head extremities of lutein or along the polyene chain. A simulation of these cases has been performed and the outcome is shown in Figure 6.

Simulations and calculations performed on 2:1 CD/lutein complexes show that all four cases are energetically favored equally (Table 3). The case showing both  $\beta$ CD molecules close to the central methyl groups—i.e. close to the center of the lutein molecule—is interesting since important CD-CD interactions are possible between the short-distanced CD molecules. Those are wrapping around the lutein molecule more closely compared to the 1:1 case, enhancing the intermolecular interaction energy between lutein and  $\beta$ CD, from  $-16.91$  kcal/mol with one  $\beta$ CD to  $-19.3$  kcal/mol with two  $\beta$ CDs (Table 3). The other structures are characterized by lower CD-CD interactions due to a larger distance separating them. Thus, intermolecular interactions between lutein and  $\beta$ CD are similar between 1:1 and 2:1 structures with the same initial position of  $\beta$ CD, which is in accordance with the modeling work of Nalawade and Gajjar.<sup>23</sup>

**3.2. Modeling of Cyclodextrin Crystals and Study of Carotenoid Adsorption on the Crystal Faces.** As summarized in Figure 1, depending on the process pathways followed to produce the cyclodextrin/bioactive complex, CD may remain in a solid crystalline form. In that case, the investigation of the interactions between the cyclodextrin and the bioactive molecule can be conducted by the estimation of adsorption energies, considering the adsorption of the bioactive molecule on each face of the cyclodextrin crystals. The adsorption phenomenon depends on the chemical affinity between the bioactive molecule and the crystal surface. The prediction of intermolecular interactions governing this affinity can be addressed using molecular modeling with the GenMol software. Crystals of cyclodextrins were modeled, and each flat face was considered separately. Then, an adsorption simulation was performed for each solute-face couple, which led to different interaction energies, providing a prediction of how likely a solute molecule is to stay adsorbed onto a given face.

In this study, the crystals of  $\beta$ CD and M- $\beta$ CD have been first built *in vacuo*, without taking into account any environment, using the attachment energy model described above. Once the crystals were built, exhibiting different crystalline faces, the

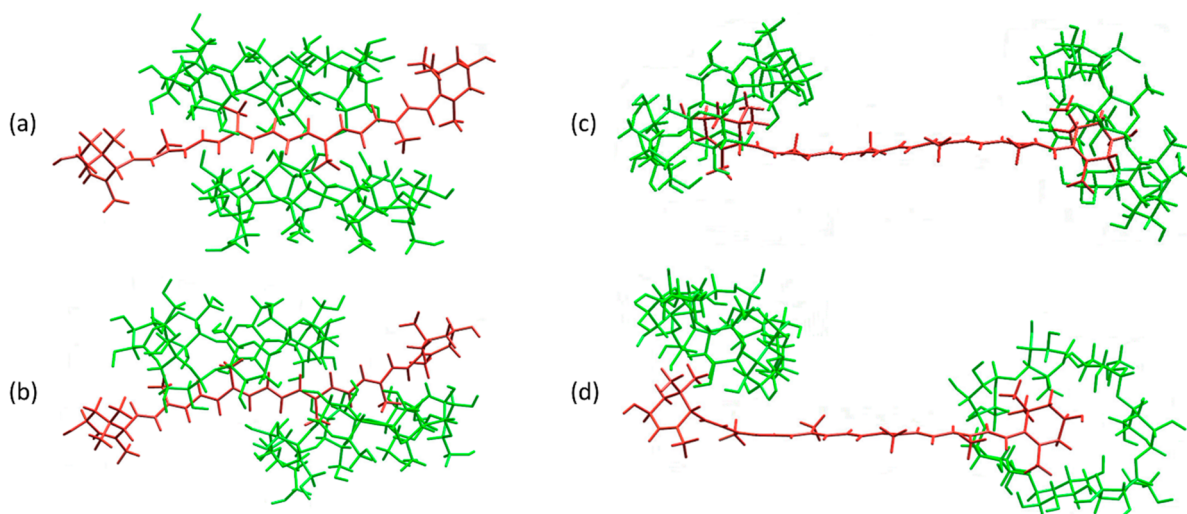


**Figure 6.** 2:1  $\beta$ CD/lutein noninclusion complexes interacting with (a) the central-most methyl group, (b) two successive methyl groups, (c) the dimethyl group on the cyclic head, and (d) the hydroxyl group.

**Table 4.** Data of Used Cyclodextrin Crystal References

CSD ref. code	Proposed name	Molecules per crystal lattice	Space group	Lattice parameters
GAKPOA	BC9	2 $\beta$ CD + 9 H <sub>2</sub> O	Monoclinic $P2_1$	$a = 15.1417 \text{ \AA}$ $b = 10.1840 \text{ \AA}$ $c = 20.937 \text{ \AA}$ $\beta = 110.926^\circ$
BCDEXD10	BC13	2 $\beta$ CD + 13 H <sub>2</sub> O	Monoclinic $P2_1$	$a = 21.29 \text{ \AA}$ $b = 10.33 \text{ \AA}$ $c = 15.10 \text{ \AA}$ $\beta = 110.926^\circ$
GEKWIF	BC15	2 $\beta$ CD + 15 H <sub>2</sub> O	Monoclinic $P2_1$	$a = 14.970 \text{ \AA}$ $b = 10.1740 \text{ \AA}$ $c = 21.298 \text{ \AA}$ $\beta = 112.366^\circ$
IQOZIX	MBC13	2 M- $\beta$ CD + 13 H <sub>2</sub> O	Orthorhombic $P2_12_12_1$	$a = 12.663 \text{ \AA}$ $b = 17.679 \text{ \AA}$ $c = 31.271 \text{ \AA}$

adsorption of lutein, lycopene, and  $\beta$ -carotene on each identified face was investigated.

Since the  $\beta$ CD crystal is unstable without water molecules, the crystallization modeling presented in this study considered water molecules being present in the crystal packing. Indeed, as mentioned above, the  $\beta$ CD crystal is more stable if the lattice is filled with a dozen water molecules.<sup>3,4</sup> To account for that reported water-dependence of the crystal stability, three  $\beta$ CD references from the CSD have been used, as well as one for M- $\beta$ CD, namely GAKPOA, BCDEXD10, GEKWIF, and IQOZIX. The molecular composition, space group, and lattice parameters are given in Table 4.

Data contained in the provided CIF files allow retrieval of the crystalline packing and build the crystal with the attachment energy model. For each reference, a list of about 20 probable faces was proposed, for which the attachment energy, and thus the linear growth rate, was calculated. Only the apparent faces were kept for further calculations, namely the slow growing ones, hence the ones with the higher  $E_{\text{att}(hkl)}$ . Table 5 shows the cyclodextrin crystal habits *in vacuo*, the calculated crystal energy,  $E_{\text{cr}}$ , and the attachment energies for each  $(hkl)$  face,  $E_{\text{att}(hkl)}$ .

**Table 5.** Attachment Energies and Interaction Energies between Carotenoids and  $\beta$ CD and M- $\beta$ CD

	$E_{\text{cr}}$ (kcal/mol)	(h k l)	$E_{\text{att}(hkl)}$ (kcal/mol)	$E_{\text{i}(hkl)}$ (kcal/mol)			Crystal habit <i>in vacuo</i>
				Lutein	Lycopene	$\beta$ -Carotene	
BC9	-77.8	0 0 1	-4.65	-23.4	-22.4	-22.6	
		1 0 -1	-6.9	-24	-23.6	-24.6	
		1 0 0	-8.9	-21.8	-25	-21.9	
		1 -1 0	-23.8	-24.4	-21.6	-26.1	
		0 -1 -1	-24.4	-20.8	-20.4	-20.4	
		0 1 1	-25	-22.6	-23	-23	
		1 1 0	-25.1	-23.6	-23.9	-22.5	
BC13	-136	1 0 0	-20.5	-24.8	-25	-24.4	
		0 0 1	-30.5	-25.1	-26	-24	
		1 0 -1	-35.1	-24.3	-24.9	-25.3	
		1 -1 0	-51.3	-23.7	-22.1	-26.4	
		1 1 0	-51.6	-24.6	-23.2	-21.7	
BC15	-123	0 0 1	-13.7	-27.1	-22.6	-23.7	
		1 0 0	-18.3	-24.5	-27	-25	
		1 0 -1	-21.3	-24.1	-24.6	-26.2	
		0 1 1	-33.4	-22.3	-23.4	-25	
MBC13	-128	0 1 -1	-15.9	-26.3	-23.6	-25.2	
		0 0 -2	-16.3	-23.5	-27.9	-26.5	
		1 0 -2	-20.3	-24	-23.1	-22.2	
		1 0 -1	-32.0	-22.5	-20.1	-21.7	
		1 0 -2	-33.9	-21.5	-18.5	-17.5	
		1 1 0	-34.7	-19.5	-17.9	-18.4	

Adsorption energies,  $E_{\text{i}(hkl)}$ , were calculated for lutein, lycopene, and  $\beta$ -carotene on each face of the  $\beta$ CD and M-



$\beta$ CD crystals and are provided alongside the corresponding attachment energy,  $E_{\text{att}(hkl)}$  in Table 5. When these two energies are compared to one another, one can deduce the interaction behavior:<sup>41,42</sup> if  $E_{i(hkl)} < E_{\text{att}(hkl)}$ ; then the interaction of the molecule is significant and can disrupt the growth of a given face, whereas if  $E_{i(hkl)} > E_{\text{att}(hkl)}$ , this hindrance most likely will not happen. An example of the adsorption simulation outcome is provided in Figure 7 for the case of the adsorption of a lutein molecule on the (001) face of BC9, at thermodynamic equilibrium.

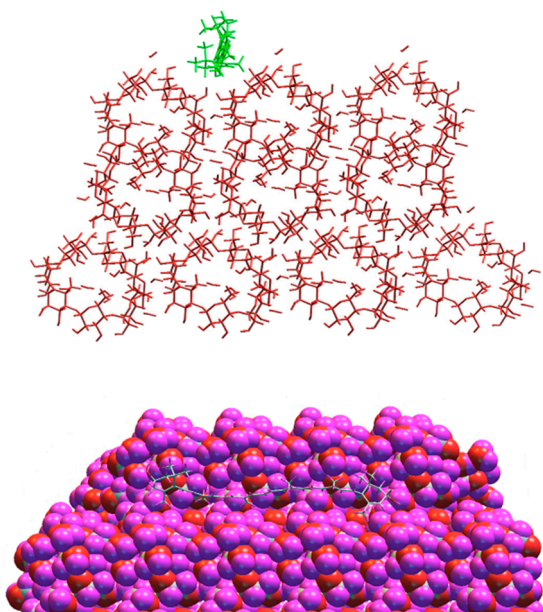


**Figure 7.** Different representations of the outcome of the adsorption simulation for the case of the adsorption of a lutein molecule on the (001) face of BC9.

#### 4. DISCUSSION

In general, numerous studies reported in the literature on the use of CD as a carrier for drugs and bioactives refer to the final product as an inclusion complex without considering the possibilities of noninclusion complexes or that the CD can be in crystalline form. The processing steps employed dictate whether the CD is dispersed enough to be able to form inclusion complexes (Figure 1). In addition, the molecular size of the drug/bioactive and the different groups on the molecule dictate the extent of interactions and which part of the molecule can fit into the cavity of the specific CD used; however, this aspect is also often not considered. Considering carotenoids as model bioactives, this study evaluated different cases of noninclusion complexes as well as adsorption on crystal faces of different types of CD using molecular modeling approaches.

According to the results shown in Table 5 for the three different water contents of  $\beta$ CD (BC9, BC13, and BC15 with respectively 9, 13, and 15 water molecules per lattice), the most stable crystal is the one with 13 water molecules with  $E_{\text{cr}} = -136$  kcal/mol. Furthermore, with the same number of water molecules in the crystal lattice,  $\beta$ CD is more stable than M- $\beta$ CD with  $E_{\text{cr}} = -128$  kcal/mol.

The predicted crystal habit *in vacuo*, using the attachment energy model (Table 5), shows that the habit of BC9 is flat and

elongated with large (001) and (10-1) faces, while for BC13 and BC15, it tends toward an isometric shape. Both predicted habits are very close to one another, where only the indexation of faces differs as the crystal lattice was considered in different space coordinates. Therefore, for instance, the (100) face of BC13 is the same as the (001) face of BC15. Finally, the habit of MBC13, which has the only orthorhombic packing of this selection, exhibits a prismatic habit with a length about two times as long as its thickness.

As for the interaction energies, they are close to one another in most cases, independent of the nature of the carotenoid solute, the cyclodextrin crystal considered (especially the water content), and the crystal face considered. Depending on those two parameters, the interaction energies range from -17.5 to -27.9 kcal/mol, with most cases ranging from -20 to -25 kcal/mol. This can be explained as solutes are chemically close to one another within the carotenoid family with lutein being oxygenated as opposed to lycopene and  $\beta$ -carotene. Likewise, cyclodextrin molecules are cyclic and highly symmetric, and every one of the crystal faces are therefore exhibiting similar chemical compositions, varying only in the structural organization of the cyclodextrin molecules. As a matter of fact, this atomic scale rugosity does not favor a selective adsorption of the tested carotenoids, with the latter being too elongated to take advantage of the asperities created by the crystal packing. The water content does not seem to affect this interaction either, since the average calculated interaction energies, with each carotenoid, are of the same order of magnitude for all the considered crystal structures with 9, 13, or 15 waters per crystal lattice. Water-carotenoid interactions are low, which is a consequence of the spreading of water molecules. The majority of the calculated intermolecular interactions are due to cyclodextrin-carotenoid interactions rather than water-carotenoid interactions, even at higher water contents.

This overall similarity of carotenoid interactions on CD crystal faces leads to the conclusion that face growths are equally impacted due to adsorption effects. The crystal face growth rates are not significantly modified relative to one another; therefore, the crystal habit shall not be modified either if the crystal structure remains the same. However, the current results, highlighting the chemical affinities between the carotenoids and the CD crystals, do not allow the prediction of whether this adsorption effect can result in an important loading of carotenoids at the surface of CD crystals.

#### 5. CONCLUSION

The characteristics of cyclodextrin/carotenoid complexes have been investigated by molecular modeling, focusing on the complexes formed either between dispersed molecules of cyclodextrins and carotenoids or between cyclodextrin crystals and carotenoids. For the case of dispersed cyclodextrin molecules, lutein was chosen as the carotenoid model molecule. The modeling of its complexation with five different cyclodextrins exhibited different types of preferential interactions depending mainly on the CD size and steric hindrance. The strongest interactions of the smallest CD molecule studied,  $\alpha$ CD, with lutein have been highlighted to be with one methyl group of the polyene chain while  $\beta$ CD, M- $\beta$ CD, and HP- $\beta$ CD can have strong interactions with two successive methyl groups, the dimethyl group as well as the cyclic head. Lastly, the biggest CD molecule studied,  $\gamma$ CD, would be placed preferentially close to the cyclic head, with the strongest

interaction being along the dimethyl group, almost in parallel with the cyclic head. In any case, due to the size of the lutein molecule, a complete inclusion in the host CD molecule is not possible for the different pairs of CD/lutein considered. These modeling results give useful information for the characterization of these noninclusion CD/lutein complexes formed from dispersed cyclodextrin and lutein molecules.

The second modeling work focused on the crystal habits with the apparent faces of  $\beta$ CDs ( $\beta$ CD with different water contents) and M- $\beta$ CD, as well as the adsorption of lutein, lycopene, and  $\beta$ -carotene on the different faces. Whatever the nature of the CD, the number of water molecules for the CD, and the nature of the adsorbed carotenoid molecule, the adsorption energies were of the same order of magnitude. This result is due to the similarity of the three carotenoid molecules studied and to the fact that the water-carotenoid interactions are weak.

The modeling work performed here gives relevant elements on the interactions that will be involved during the formation of cyclodextrin/carotenoid complexes, depending on the pathway followed during the formation process, depending on whether or not the cyclodextrin has been molecularly dispersed. Further experimental studies are required to validate the results obtained and to determine the extent of loading that can be obtained for the different complexes evaluated. In addition, similar molecular modeling approaches can be extended to study bioactives/drugs of different chemical classes to demonstrate the versatility of such approaches, which will lead to the selection of the best carrier for a given bioactive/drug based on a fundamental understanding of their molecular interactions prior to embarking on lengthy trials of experimentally testing each possible combination.

## ■ ACKNOWLEDGMENTS

F. Temelli is grateful for the financial support provided to her by the Aix-Marseille University during her sabbatical leave from the University of Alberta. S. Clercq thanks Gérard Pèpe for the availability of GenMol and the knowledge he shared with us.

## ■ REFERENCES

- (1) Loftsson, T.; Brewster, M. E. Pharmaceutical applications of cyclodextrins. 1. Drug solubilization and stabilization. *J. Pharm. Sci.* **1996**, *85*, 1017–1025.
- (2) Sabadini, E.; Cosgrove, T.; Egídio, F. C. Solubility of cyclomaltooligosaccharides (cyclodextrins) in H<sub>2</sub>O and D<sub>2</sub>O: a comparative study. *Carbohydr. Res.* **2006**, *341* (2006), 270–274.
- (3) Ivanova, B.; Spitter, M. Macromolecular ensembles of cyclodextrin crystallohydrates and clathrates – experimental and theoretical gas – and condense phase study. *Int. J. Biol. Macromol.* **2014**, *64*, 383–391.
- (4) Crini, G.; Fourmentin, S.; Fenyvesi, E.; Torri, G.; Fourmentin, M.; Morin-Crini, N. Fundamentals and applications of cyclodextrins. In *Cyclodextrin Fundamentals, Reactivity and Analysis*; Fourmentin, S., et al., Eds.; Environmental Chemistry for a Sustainable World, Springer International Publishing AG, 2018; Ch. 1, pp1–55. DOI: [10.1007/978-3-319-76159-6\\_1](https://doi.org/10.1007/978-3-319-76159-6_1).
- (5) Saenger, W.; Jacob, J.; Gessler, K.; Steiner, T.; Hoffmann, D.; Sanbe, H.; Koizumi, K.; Smith, S. M.; Takaha, T. Structures of the common cyclodextrins and their larger analogues-beyond the doughnut. *Chem. Rev.* **1998**, *98* (1998), 1787–1802.
- (6) He, Y.; Fu, P.; Shen, X.; Gao, H. Cyclodextrin-based aggregates and characterization by microscopy. *Micron* **2008**, *39*, 495–516.
- (7) Messner, M.; Kurkov, S. V.; Jansook, T.; Loftsson, T. Self-assembled cyclodextrin aggregates and nanoparticles. *Int. J. Pharm.* **2010**, *387*, 199–208.
- (8) Ozdemir, N.; Pola, C. C.; Teixeira, B. N.; Hill, L. E.; Bayrak, A.; Gomes, C. L. Preparation of black pepper oleoresin inclusion complexes based on beta-cyclodextrin for antioxidant and antimicrobial delivery applications using kneading and freeze drying methods: A comparative study. *LWT - Food Science and Technology* **2018**, *91*, 439–445.
- (9) Babaglu, H. C.; Bayrak, A.; Ozdemir, N.; Ozgun, N. Encapsulation of clove essential oil in hydroxypropyl beta-cyclodextrin for characterization, controlled release, and antioxidant activity. *J. Food Process. Preserv.* **2017**, *41*, DOI: [10.1111/jfpp.13202](https://doi.org/10.1111/jfpp.13202).
- (10) Li, D.; Wu, H.; Huang, W.; Guo, L.; Dou, H. Microcapsule of sweet orange essential oil encapsulated in beta-cyclodextrin improves the release behaviors in vitro and in vivo. *Eur. J. Lipid Sci. Technol.* **2018**, *120*, DOI: [10.1002/ejlt.201700521](https://doi.org/10.1002/ejlt.201700521).
- (11) Ahmad, M.; Ashraf, B.; Gani, A. Microencapsulation of saffron anthocyanins using glucan and cyclodextrin: Microcapsule characterization, release behaviour & antioxidant potential during in-vitro digestion. *Int. J. Biol. Macromol.* **2018**, *109*, 435–442.
- (12) López-Nicolás, J. M.; Rodríguez-Bonilla, P.; García-Carmona, F. Cyclodextrins and antioxidants. *Crit. Rev. Food Sci. Nutr.* **2014**, *54*, 251–276.
- (13) Kaiser, A.; Haskins, C.; Siddiqui, M. M.; Hussain, A.; D'Adamo, C. The evolving role of diet in prostate cancer risk and progression. *Curr. Opin. Oncol.* **2019**, *31*, 222–229.
- (14) Frede, K.; Ebert, F.; Kipp, A. P.; Schwerdtle, T.; Baldermann, S. Lutein activates the transcription factor Nrf 2 in human retinal pigment epithelial cells. *J. Agric. Food Chem.* **2017**, *65*, 5944–5952.
- (15) Al-Marzouqi, A. H.; Jobe, B.; Dowaidar, A.; Maestrelli, F.; Mura, P. Evaluation of supercritical fluid technology as preparative technique of benzocaine-cyclodextrin complexes - Comparison with conventional methods. *J. Pharm. Biomed. Anal.* **2007**, *43*, 566–574.
- (16) Al-Marzouqi, A. H.; Jobe, B.; Corti, G.; Cirri, M.; Mura, P. Physicochemical characterization of drug-cyclodextrin complexes prepared by supercritical carbon dioxide and by conventional techniques. *J. Inclusion Phenom. Macrocyclic Chem.* **2007**, *57*, 223–231.
- (17) Al-Marzouqi, A. H.; Solieman, A.; Shehadi, I.; Adem, A. Influence of the preparation method on the physicochemical properties of econazole- $\beta$ -cyclodextrin complexes. *J. Inclusion Phenom. Mol. Recognit. Chem.* **2008**, *60*, 85–93.
- (18) Temelli, F. Perspectives on the use of supercritical particle formation technologies for food ingredients. *J. Supercrit. Fluids* **2018**, *134*, 244–251.
- (19) González-Gaitano, G.; Rodríguez, P.; Isasi, J. R.; Fuentes, M.; Tardajos, G.; Sánchez, M. The aggregation of cyclodextrins as studied by photon correlation spectroscopy. *J. Inclusion Phenom. Mol. Recognit. Chem.* **2002**, *44*, 101–105.

- (20) Loftsson, T.; Saokham, P.; Couto, A. R. S. Self-association of cyclodextrins and cyclodextrin complexes in aqueous solutions. *Int. J. Pharm.* **2019**, *560*, 228–234.
- (21) Szente, L.; Szejtli, J.; Kis, G. L. Spontaneous opalescence of aqueous  $\gamma$ -cyclodextrin solutions: Complex formation or self-aggregation. *J. Pharm. Sci.* **1998**, *87*, 778–781.
- (22) Loftsson, T.; Másson, M.; Brewster, M. E. Self-Association of Cyclodextrins and Cyclodextrin Complexes. *J. Pharm. Sci.* **2004**, *93*, 1091–1099.
- (23) Nalawade, P.; Gajjar, A. Preparation and characterization of spray dried complexes of lutein with cyclodextrins. *J. Inclusion Phenom. Macrocyclic Chem.* **2015**, *83*, 77–87.
- (24) Zhao, Q.; Miriyala, N.; Su, Y.; Chen, W.; Gao, X.; Shao, L.; Yan, R.; Li, H.; Yao, X.; Cao, D.; Wang, Y.; Ouyang, D. Computer-aided formulation design for a highly soluble lutein-cyclodextrin multiple-component delivery system. *Mol. Pharmaceutics* **2018**, *15*, 1664–1673.
- (25) Faucci, M. T.; Melani, F.; Mura, P. <sup>1</sup>H-NMR and molecular modelling techniques for the investigation of the inclusion complex of econazole with  $\alpha$ -cyclodextrin in the presence of malic acid. *J. Pharm. Biomed. Anal.* **2000**, *7*.
- (26) Gurikov, P.; Smirnova, I. Amorphization of drugs by adsorptive precipitation from supercritical solutions: A review. *J. Supercrit. Fluids* **2018**, *132*, 105–125.
- (27) Van Hees, T.; Piel, G.; Henry de Hassonville, S.; Evrard, B.; Delattre, L. Determination of the free/included piroxicam ratio in cyclodextrin complexes: comparison between UV spectrophotometry and differential scanning calorimetry. *European Journal of Pharmaceutical Sciences* **2002**, *15*, 347–353.
- (28) Lai, S.; Locci, E.; Piras, A.; Porcedda, S.; Lai, A.; Marongiu, B. Imazalil–cyclomaltoheptaose ( $\beta$ -cyclodextrin) inclusion complex: preparation by supercritical carbon dioxide and <sup>13</sup>C CPMA and <sup>1</sup>H NMR characterization. *Carbohydr. Res.* **2003**, *338*, 2227–2232.
- (29) Türk, M.; Upper, G.; Steurethaler, M.; Hussein, Kh.; Wahl, M. A. Complex formation of Ibuprofen and  $\beta$ -Cyclodextrin by controlled particle deposition (CPD) using SC-CO<sub>2</sub>. *J. Supercrit. Fluids* **2007**, *39*, 435–443.
- (30) National Toxicology Program, Institute of Environmental Health Sciences, National Institutes of Health (NTP). 1992. National Toxicology Program Chemical Repository Database. Research Triangle Park, NC.
- (31) Thurein, S. M.; Nutdanai, L.; Thawatchai, P. Physicochemical Properties of  $\beta$ -Cyclodextrin Solutions and Precipitates Prepared from Injectable Vehicles. *Asian J. Pharmaceutical Sci.* Special Issue: Pharmaceutical Innovation, *13*, no. 5 (September 1, 2018): 438–49. DOI: [10.1016/j.ajps.2018.02.002](https://doi.org/10.1016/j.ajps.2018.02.002).
- (32) Negi, J. S.; Chattopadhyay, P.; Sharma, A. K.; Ram, V. Preparation of gamma cyclodextrin stabilized solid lipid nanoparticles (SLNS) using stearic acid– $\gamma$ -cyclodextrin inclusion complex. *J. Inclusion Phenom. Macrocyclic Chem.* **2014**, *80*, 359–368.
- (33) Pathak, S. M.; Musmade, P.; Dengle, S.; Karthik, A.; Bhat, K.; Udupa, N. Enhanced oral absorption of saquinavir with Methyl-Beta-Cyclodextrin—Preparation and in vitro and in vivo evaluation. *Eur. J. Pharm. Sci.* **2010**, *41*, 440–451.
- (34) Saokham, P.; Muankaew, C.; Jansook, P.; Loftsson, T.; Solubility of Cyclodextrins and Drug/Cyclodextrin Complexes. *Molecules* **2018**, *23*, DOI: [10.3390/molecules23051161](https://doi.org/10.3390/molecules23051161).
- (35) Suta, L. M.; Vlaia, L.; Fulas, A.; Ledeti, I.; Hadaruga, D.; Mircioiu, C. Evaluation Study of the Inclusion Complexes of Some Oxicams with 2-hydroxypropyl- $\beta$ -cyclodextrin. *Revista de Chimie -Bucharest- Original Edition-*. **2013**, *64*, 1279–1283.
- (36) Grulke, C. M.; Williams, A. J.; Thillanadarajah, I.; Richard, A. M. EPA's DSSTox database: History of development of a curated chemistry resource supporting computational toxicology research. *Computational Toxicology* **2019**, *12*, 100096.
- (37) Del Re, G. 812. A simple MO–LCAO method for the calculation of charge distributions in saturated organic molecules. *J. Chem. Soc.* **1958**, *0*, 4031–4040.
- (38) Pèpe, G.; Serres, B.; Laporte, D.; Del Re, G.; Minichino, C. Potentials on Macromolecules in a Monopole Approximation: A Computer Program and an Application to Cytochromes. *J. Theor. Biol.* *115*, no. 4 (August 21, 1985): 571–93. DOI: [10.1016/S0022-5193\(85\)80141-7](https://doi.org/10.1016/S0022-5193(85)80141-7).
- (39) Pèpe, G.; Perbost, R.; Courcambeck, J.; Jouanna, P. Prediction of molecular crystal structures using a genetic algorithm: Validation by GenMol™ on energetic compounds. *J. Cryst. Growth* **2009**, *311*, 3498–3510.
- (40) Hartman, P.; Bennema, P. The attachment energy as a habit controlling factor. *J. Cryst. Growth* **1980**, *49*, 145–156.
- (41) Pèpe, G.; Fery-Forgues, S.; Jouanna, P. Predicting crystal structure and habit of organic micro-crystals by experimentally assisted molecular modelling (EAMM). The case of n-octylamino-NBD. *J. Cryst. Growth* **2011**, *333*, 25–35.
- (42) Clercq, S.; Mouahid, A.; Pèpe, G.; Badens, E. Prediction of Crystal–Solvent Interactions in a Supercritical Medium: A Possible Way to Control Crystal Habit at High Supersaturations with Molecular Modeling. *Cryst. Growth Des.* **2020**, *20*, 6863–6876.